HHS Public Access

Author manuscript

Pediatr Radiol. Author manuscript; available in PMC 2021 October 01.

Published in final edited form as:

Pediatr Radiol. 2020 October ; 50(11): 1594–1601. doi:10.1007/s00247-020-04743-9.

Connectome mapping with edge density imaging differentiates pediatric mild traumatic brain injury from typically developing controls: proof of concept

Cyrus A. Raji[1,2], **Maxwell B. Wang**[1], **NhuNhu Nguyen**[1], **Julia P. Owen**[1], **Eva M. Palacios**[1], **Esther L. Yuh**[1], **Pratik Mukherjee**[1]

[1]Neural Connectivity Laboratory, Department of Radiology and Biomedical Imaging, University of California, San Francisco, 185 Berry St., Suite 350, San Francisco, CA 94158, USA

[2]Mallinckrodt Institute of Radiology, Division of Neuroradiology, Washington University in St. Louis, St. Louis, MO, USA

Abstract

Background—Although acute neurologic impairment might be transient, other long-term effects can be observed with mild traumatic brain injury. However, when pediatric patients with mild traumatic brain injury present for medical care, conventional imaging with CT and MR imaging often does not reveal abnormalities.

Objective—To determine whether edge density imaging can separate pediatric mild traumatic brain injury from typically developing controls.

Materials and methods—Subjects were recruited as part of the “Therapeutic Resources for Attention Improvement using Neuroimaging in Traumatic Brain Injury” (TRAIN-TBI) study. We included 24 adolescents (χ=14.1 years of age, σ=1.6 years, range 10–16 years), 14 with mild traumatic brain injury (TBI) and 10 typically developing controls. Neurocognitive assessments included the pediatric version of the California Verbal Learning Test (CVLT) and the Attention Network Task (ANT). Diffusion MR imaging was acquired on a 3-tesla (T) scanner. Edge density images were computed utilizing fiber tractography. Principal component analysis (PCA) and support vector machines (SVM) were used in an exploratory analysis to separate mild TBI and control groups. The diagnostic accuracy of edge density imaging, neurocognitive tests, and fractional anisotropy (FA) from diffusion tensor imaging (DTI) was computed with two-sample *t*-tests and receiver operating characteristic (ROC) metrics.

Results—Support vector machine–principal component analysis of edge density imaging maps identified three white matter regions distinguishing pediatric mild TBI from controls. The bilateral tapetum, sagittal stratum, and callosal splenium identified mild TBI subjects with sensitivity of

Cyrus A. Raji, cyrusraji@gmail.com.

Conflicts of interest None

79% and specificity of 100%. Accuracy from the area under the ROC curve (AUC) was 94%. Neurocognitive testing provided an AUC of 61% (CVLT) and 71% (ANT). Fractional anisotropy yielded an AUC of 48%.

Conclusion—In this proof-of-concept study, we show that edge density imaging is a new form of connectome mapping that provides better diagnostic delineation between pediatric mild TBI and healthy controls than DTI or neurocognitive assessments of memory or attention.

Keywords

Brain; Children; Concussion; Diffusion tensor imaging; Edge density imaging; Magnetic resonance imaging; Traumatic brain injury

Introduction

Pediatric mild traumatic brain injury (TBI) is a major global public health problem, affecting up to 280 children per 100,000 on an annual basis and 475,000 children in the United States per year, resulting in 7,000 deaths and 60,000 hospitalizations [1]. Within the United States, falls are the most common cause, followed by motor vehicle collisions [2]. Recreational and team youth sports such as American football and hockey are also an increasingly discussed cause of pediatric concussions [3]. Concussion represents a head injury that leads to impairment of neurologic function, also known as mild TBI [4]. While acute neurologic impairment might be transient, other long-term effects can be observed with mild TBI. History of mild TBI in the pediatric population relates to impaired cognition [5], sleep disorders [6], and psychiatric afflictions such as post-traumatic stress disorder and obsessive compulsive disorder [5, 7].

When children with mild TBI present for medical care, conventional imaging with CT and MR imaging often does not reveal abnormalities. One study of 105 children who presented with acute mild TBI and received CT imaging on the day of injury and conventional MRI within 2 weeks demonstrated only a 15% detection rate of abnormal findings with CT and 34% with conventional MRI [8].

Subtle mild TBI abnormalities not visualized on CT or conventional MRI can be detected with advanced neuroimaging techniques. One such method is diffusion MR imaging [9], which allows for qualitative and quantitative assessment of specific white matter tracts in the brain. This modality has particular relevance to mild TBI because of the associated white matter damage that occurs at a microstructural level from rotational, stretching and shearing forces [10]. In a separate study of pediatric mild TBI cases scanned within 96 h of injury, increased fractional anisotropy (FA) was shown in the middle temporal gyrus, superior temporal gyrus, anterior corona radiata, and superior longitudinal fasciculus [11]. These findings are consistent with a meta-analysis of 20 studies that reported a trend of increased FA 4 weeks post injury but decreased FA 3 months post injury [12]. This same study also linked FA values to cognitive scores at 4 weeks post injury [12].

Additional potential exists to extract sensitive metrics of mild TBI from diffusion MR imaging under the paradigm of the structural connectome: a network of white matter

connections containing hubs of particularly strong connectivity in the brain [13]. While FA is a robust parameter of microstructure in isolated large white matter tracts, it does not directly assess inter-regional connectivity and it can fail to capture complex details involving crossing fibers or subresolution structural differences [14, 15]. Therefore, diffusion tractography has been proposed as an alternative for assessing white matter integrity through the use of track density imaging and edge density imaging [15–19]. In particular, because of its focus on connectomics, edge density imaging has been shown to correspond well to patterns identified with other network analytic approaches such as rich club analysis, network communicability and network eigenmodes [20, 21]. If edge density imaging demonstrated abnormalities in mild TBI, it could change patient management by providing more sensitive diagnosis because a key obstacle in the care of these children is diagnosing them at subtler levels of injury.

We hypothesized that edge density imaging can serve as a diagnostic biomarker for white matter injury in children with mild TBI. The present study serves to formally characterize distinguishable patterns of edge density imaging in healthy development and in chronic mild TBI, particularly in cases where a lack of sensitivity of CT and conventional MRI can result in symptomatic patients with negative imaging results.

Materials and methods

Subjects

With institutional review board approval and Health Insurance Portability and Accountability Act (HIPAA) adherence, pediatric subjects were recruited for the "Therapeutic Resources for Attention Improvement using Neuroimaging in Traumatic Brain Injury" (TRAIN-TBI) study. Fourteen children with mild TBI diagnosis, based on Glasgow coma scale (GCS) score of 14/15 or 15/15, were prospectively enrolled. Because the focus of this study was to examine residual long-term changes caused by traumatic brain injury (TBI), the study does not pertain to the acute phase and participants were excluded if it had been less than 1 month since TBI. Besides GCS score, the inclusion and exclusion criteria for the study were: (a) ages 8–16 years old, (b) sustained blunt TBI at least 1 month prior to enrollment date, (c) currently experiencing at least one post-concussion symptom at the time of enrollment, and (d) had no previous neurologic or psychiatric medical history such as migraine headaches or depression. Post-concussion symptoms were determined by the Rivermead Post-Concussion Symptoms Questionnaire (RPQ) [20] and the Glasgow Outcome Scale–Extended Pediatric (GOSEP) [21] tests. Ten children matched in age, handedness and education with no history of mild TBI were recruited as a control group. Gender was a separate co-variate in all statistical analyses. All subjects underwent neurocognitive evaluations with the pediatric version of the California Verbal Learning Test (CVLT) [22] and the Attention Network Task (ANT) [23]. Two-sample *t*-tests were performed in SPSS Statistics (version 24; IBM, Armonk, NY) to compare demographic characteristics and cognitive tests between the pediatric mild TBI and control groups.

Magnetic resonance imaging acquisition

A 3-T GE MR750 scanner (GE Healthcare, Waukesha, WI) was used to perform MRI using a 32-channel phased-array radiofrequency head coil. High-resolution structural MRI of the brain was collected using an axial 3-D BRAVO T1-weighted sequence (repetition time [TR]/ echo time [TE]/inversion time [TI] = 6.6/1.64/400 ms, flip angle 11°) with a 256-mm field of view (FOV), and 160 1.2-mm contiguous partitions at a 256×256 matrix. Whole-brain diffusion tensor imaging (DTI) was performed with a multi-slice single-shot spin-echo planar pulse sequence (TR/TE 6.7/80.4 ms) using 64 diffusion-encoding directions, isotropically distributed over the surface of a sphere with electrostatic repulsion acquired at b = 1,300 s/mm^2, eight acquisitions at b = 0 s/mm^2; interleaved slices of 2.7-mm thickness, each with no gap between slices; a 128×128 matrix; FOV of 350×350 mm; and ASSET (array spatial sensitivity encoding technique) parallel imaging with acceleration factor R=2. For clinical neuroradiology evaluations, non-contrast T1-, T2-, T2- fluid-attenuated inversion recovery (FLAIR), diffusion-, and gradient echo T2*-weighted images were assessed by board-certified neuroradiologists with certificates of added qualification in neuroradiology (E.L.Y., with 5 years of experience, and P.M., with 12 years of experience). The purpose of these evaluations was to document any visually identifiable abnormality including those detailed in the National Institutes of Health (NIH) common data elements for traumatic brain injury [24], such as visually identifiable brain atrophy or encephalomalacia, evidence of prior hemorrhage, or white matter damage.

Diffusion magnetic resonance imaging analyses

Diffusion MRI data were preprocessed and analyzed in the FMRIB (functional magnetic resonance imaging of the brain) Software Library (FSL, version 5.0.7; Analysis Group, FMRIB, Oxford, UK). Motion-artifact-degraded diffusion MR images were excluded from all analyses. Non-brain tissue was first removed using the brain extraction tool with a fractional intensity threshold of 0.3 [25]. Diffusion-weighted images were corrected for motion and eddy currents using the FMRIB linear-image registration tool [26], which uses the default options of a normalized correlation cost function for intra-modal registration with 6° of freedom, a multi-start course search for optimization, and trilinear interpolation, with b = 0 s/mm^2 image as the reference. Fractional anisotropy maps were computed using FSL's DTIFit tool.

Connectome mapping with edge density imaging

Edge density images were computed as described in [18]. The T1-weighed MR images were segmented using FreeSurfer 5.3.0 [27] and the Desikan-Killiany parcellation into 68 cortical and 14 subcortical regions [28]. Bedpostx [29] was run to estimate the fiber orientations at every voxel. Probabilistic fiber tractography was performed with probtrackx2 [29] between each possible pair of regions, with each white matter connection between a pair of regions constituting an "edge," which is graph theory terminology for a network connection. The directed edge path was defined as the top 95% of non-zero voxels by streamline count. To form a bidirectional edge, the union of both directed edges was taken. Spurious edges were removed by utilizing the consensus connectome computed in Owen et al. [19]. The edge density of a voxel was then defined as the number of edges that passed through the voxel.

Tract-based statistics

To identify trends in FA and edge density in mild TBI, we first observed how those metrics changed in individual tracts. Specifically, we averaged the imaging metric of interest (FA or edge density) across each of the 48 Johns Hopkins University (JHU) atlas [30] regions and calculated a two-sample *t*-test between the mild TBI and control groups. We then corrected results for multiple comparisons using the Benjamini–Hochberg procedure [31] at a false discovery rate of 0.05. We also analyzed mean diffusivity and axial diffusivity in the same manner.

Dimensionality reduction and preliminary support vector machine–principal component analysis

Using the FMRIB linear-image registration tool, each edge density imaging map was registered to MNI152 space [32] and averaged across each JHU tract. We used principal component analysis (PCA) [33] and support vector machines (SVM) using linear kernels [34] to identify changes in the mean edge density of the 48 JHU atlas [30] white matter tracts at the subject level for preliminary binary classification purposes. The PCA components explaining the largest amount of variance were used as features in the SVM. Hyperparameters, such as the number of PCA components used or regularization weighting, were determined using nested leave-one-out cross-validation.

We validated our approach using receiver operating characteristic (ROC) analysis [35] and leave-one-out cross-validation to address involving imaging metric variability, multiple comparisons, and overfitting concerns [36]. For comparison, we repeated this analysis using FA as the input feature by training a new SVM-PCA model in the exact same manner.

Intuitively, SVM creates a hyperplane to separate the mild TBI and control groups from each other, and the predictor variable for each subject was defined as the distance between the subject and this hyperplane. The sign of this distance would indicate which side of the plane the subject was on. To evaluate for statistical significance, we calculated a two-sample heteroscedastic *t*-test between the predictor variables of the control and mild TBI groups. All code to analyze edge density imaging data was developed in-house using MATLAB (version 2016b; MathWorks, Natick, MA).

We also used a voxel-level generalized linear model to identify any statistically significant voxels between controls and mild TBI groups, as previously detailed [37].

Results

In the pediatric mild TBI group, the time from injury to MR imaging assessment was on average 30.5±58.7 months. Average RPQ score was 16.7±2.9 and average GOSEP score was 6.9±0.8. With respect to mechanism of injury, 71% (10/14) had sports-related causes including soccer (4), skiing (3), basketball (1), water polo (1) and American football (1). The remaining 4 children with mild TBI sustained their injuries from road traffic accidents (2), unintentional direct head impact against an object (1), and unintentional fall from height greater than 3 feet (1).

Table 1 reports the neurocognitive test scores. No statistically significant difference was observed between the two groups on the ANT, although children with mild TBI showed trends toward higher values, indicating worse performance, on the mean reaction time, alerting and conflict subscores. With the pediatric CVLT, the group with mild TBI had statistically significant lower values, signifying worse performance, on the long delay free recall and long delay cued recall subtests, as well as for immediate recall Trials 1 to 5.

Diagnostic neuroradiology interpretations revealed abnormal findings in 43% (6/14) of the children with mild TBI. There were non-trauma-related incidental findings in 30% (3/10) of the controls. These findings are summarized in Online Supplementary Material 1. Tract-specific JHU regional analysis also did not show any statistically significant group differences in FA, mean diffusivity or axial diffusivity values between the children with mild TBI and the controls. Online Supplementary Material 2 displays both FA and edge density imaging values for these tracts.

Figure 1 illustrates the classification weights assigned to each region by the SVM-PCA algorithm, where multiplying each child's edge density in a given region with the associated weight and then summing over all regions yielded a weighted average edge density image that accurately separated controls and children with mild TBI [38]. Here, light blue regions are associated with higher edge density in controls compared to children with mild TBI. Dark blue regions are associated with the opposite. The three regions with the highest importance in weighting are the bilateral tapetum, bilateral sagittal stratum, and the splenium of the corpus callosum. Two-sample heteroscedastic *t*-tests of edge density differences between children with mild TBI and controls within those three tracts generated *P*-values of 0.07, 0.14 and 0.24, respectively. Fractional anisotropy generated *P*-values of 0.28, 0.37 and 0.23, respectively.

Figure 2 shows the results of a preliminary analysis of diagnostic accuracy from edge density imaging maps from Fig. 1 in distinguishing children with mild TBI from controls, using all 48 JHU white matter regions. The accuracy for edge density imaging was highest at 94%. Comparisons with ROC curves from FA values, and CVLT and ANT scores are also included for comparison. Two-sample *t*-tests between the SVM-PCA predictors of the mild TBI and control groups showed a *P*-value of 8×10^{-5} for edge density, $P=0.03$ for CVLT, $P=0.49$ for ANT and $P=0.60$ for FA. The effect size of the edge density group difference was 2.0, as measured by Cohen d. There was no statistically significant correlation between classification of mild TBI versus control using the SVM-PCA algorithm and time between injury and MRI scan.

Voxel-level generalized linear model analysis did not yield any significant voxels after multiple comparisons correction. This is likely because of the small sample size necessitating some form of prior dimensionality reduction.

Figure 3 shows the SVM hyperplane and classification of individual cases and controls using edge density imaging with a sensitivity of 79% and specificity of 100%. The two controls that were nearly classified as mild TBI showed incidental findings that were not specific for trauma. One child had a developmental venous anomaly on gradient echo T2* imaging,

while another had nonspecific T2/FLAIR hyperintensities in the supratentorial white matter. A third control with a pontine capillary telangiectasia was correctly classified in this category. Two of the three children with mild TBI who were incorrectly classified as controls had no abnormal imaging findings on clinical neuroradiology assessment, while the third had a linear area of susceptibility-associated signal loss in the subcortical white matter of the left superior frontal gyrus that might represent a single focus of hemorrhagic traumatic axonal injury.

Discussion

We utilized edge density imaging, a novel biomarker based on the structural connectome, to identify abnormal white matter in children with mild TBI, specifically with decreased edge density in the bilateral tapetum, sagittal stratum, and the splenium of the corpus callosum being associated with mild TBI. We interestingly also saw a variety of areas with elevated edge density in mild TBI (albeit with lower importance weighting compared to those with decreased density), particularly within the frontal areas, which is hypothetically associated with adaptive changes given the lengthy amount of time between injury and scan date for some children in this study.

Edge density imaging displayed greater sensitivity and specificity for mild TBI than did neurocognitive testing, FA and standard neuroradiology interpretations, the last of which revealed visually apparent abnormalities on a dedicated 3-T MRI protocol in less than half of mild TBI cases. It should be noted that two of the children with mild TBI demonstrated peri-atrial white matter FLAIR signal abnormalities that did overlap with the reported edge density imaging findings.

Several prior DTI studies focused on pediatric populations in mild TBI. One investigation examined 49 children with mild TBI compared to 39 controls and found reduced FA in the body and genu of the corpus callosum, frontal white matter, and left cingulum bundle [39]. Another study focused on a mixed population of mild, moderate and severe pediatric TBI cases in 41 subjects compared to 31 controls, showing widespread FA reductions in the corpus callosum [40]. A study of 14 mild TBI subjects ages 10–18 years defined by GCS score of 13–15 showed reduced FA in inferior frontal, superior frontal, and supracallosal white matter compared to 14 controls [41]. One mild TBI study with a population ages 10–38 years showed lower FA values in males [42]. While other studies have also shown abnormally low FA values in multiple white matter tracts such as the cingulum bundle, these studies focused on moderate to severe pediatric TBI populations [43–45], whereas ours examined children with mild TBI.

Abnormalities in the callosal splenium seen in our study were observed in other mild TBI subjects ages 10–50 on FA analyses with DTI [46]. These differences were also observed in severe TBI, where T2/FLAIR lesions in that area relate to worse outcomes [47]. The sagittal stratum is a complex white matter bundle containing the inferior fronto-occipital fasciculus, the inferior longitudinal fasciculus, and the posterior thalamic radiation, all connecting the occipital lobe to the rest of the brain [48]. One prior DTI study in adults showed that decreased FA in the sagittal stratum was a distinguishing feature of mild TBI compared to

severe TBI [48]. Increased FA of the sagittal stratum was observed in a pediatric group with subacute mild TBI (n=15) [48]. The tapetum, composed of the callosal splenium fibers crossing along the margins of the lateral ventricles, has been implicated as abnormal in children with mild TBI [48]. The tapetum also connects the right and left hippocampus, which itself has been shown to be atrophic in pediatric TBI [49]. Thus, tapetum abnormalities might reflect underlying hippocampal involvement in TBI. The corpus callosum, particularly the splenium, might be selectively affected by TBI because of its longitudinal course with a midline location and close adjacency to the falx leading to damage from shear forces [50]. The role of the sagittal stratum in connecting the temporal lobes to the parietal lobes might also explain its involvement in TBI because the temporal lobes are among the most commonly damaged areas [51].

Diffusion tensor imaging findings in mild TBI range from near-perfect separation of mild TBI and controls to differences that are only barely significant on a group level [11, 12]. Lack of predictive power of FA values in identifying children with mild TBI should not be seen as contrary to this trend, but rather a result of multiple factors ranging from variance in the time from injury to mild TBI definition and cause of physical injury. These factors motivate use of edge density imaging as a more sensitive metric for mild TBI diagnosis in these particularly difficult cases.

Use of edge density imaging in our study yielded 40% improvement in diagnostic AUC over the FA scalar. Added value of edge density imaging over neurocognitive testing is also important given concerns regarding the cost of neuroimaging [52] and the current barriers to adoption of DTI for mild TBI in routine clinical practice and in medicolegal settings [53]. Lack of correlation between edge density imaging and neurocognitive testing potentially suggests an underlying level of damage to the brain from mild TBI that might precede identifiable neuropsychological deficits, although the small sample size of our study limits its statistical power for determining such correlations.

Several advantages and caveats are apparent in our investigation. Previous DTI studies in children with mild TBI have primarily analyzed white matter microstructure using FA analyses, particularly through the use of tract-based spatial statistics. However, there have been methodological critiques of fractional anisotropy and tract-based spatial statistics, ranging from the problem of crossing fibers within a given white matter voxel to signal-to-noise resolution concerns [54].

One possible reason for the increased sensitivity of edge density imaging within this cohort is that much of the damage can be limited to sub-voxel changes [17, 19, 55]. Diffusion tractography has super-resolution properties [17, 19], so edge density imaging might be more sensitive to these differences. Another potential factor is the complex relationship between the brain’s structural architecture and the neural connectome. Whereas FA probes local structural changes, edge density imaging explicitly identifies how those local changes influence network-spanning connections [17, 18].

However, it is important to note that the results of our SVM-PCA analysis are preliminary and must be replicated in larger pediatric mild TBI cohorts with the sample size needed for

training, testing and validation analyses in full machine learning analysis. Chiefly, the limited sample size and lack of true external validation dataset might mask overfitting concerns. A limitation on the visual inspection of the MR brain images was the use of gradient T2* images that are less sensitive than newer susceptibility-weighted imaging used to detect axonal injury or microhemorrhages. With these limitations in mind, further studies should be conducted, especially with regard to comparing diagnostic accuracies among different methods.

While our current study was cross-sectional, the test–retest reliability of our diffusion MR imaging connectomic methods, including EDI, enabled longitudinal evaluations. An interesting future study would be to use the patterns we identify in this paper to predict patient outcomes. Presence of controls in our cohort with MR imaging abnormalities, while incidental, might have increased the probability of these subjects being misclassified, although none ultimately was.

Conclusion

In this proof-of-concept study, edge density imaging presented a promising new imaging technique for further development and application for diagnosing children with mild TBI.

Supplementary Material

Refer to Web version on PubMed Central for supplementary material.

Acknowledgments

The TRAIN-TBI project was generously supported by a gift from Dennis J. & Shannon Wong. Dr. Raji was supported by a training grant from the National Institute of Biomedical Imaging and Bioengineering (NIH T32 EB001631), administered by the UCSF Department of Radiology and Biomedical Imaging, and the American Society of Neuroradiology Boerger Research Grant. He is currently supported by additional grants from the Radiological Society of North America Research Scholar Award and WUSTL NIH KL2 Grant (KL2 TR000450 - ICTS Multidisciplinary Clinical Research Career Development Program). Dr. Mukherjee received support from the National Institute of Neurological Disorders and Stroke (NIH R01 NS060776).

References

1. Dewan MC, Mummareddy N, Wellons JC, Bonfield CM (2016) Epidemiology of global pediatric traumatic brain injury: qualitative review. World Neurosurg 91:497–509.e1 [PubMed: 27018009]
2. Alexiou G, Prodromou N, Sfakianos G (2011) Pediatric head trauma. J Emerg Trauma Shock 4:403 [PubMed: 21887034]
3. Pfister T, Pfister K, Hagel B et al. (2016) The incidence of concussion in youth sports: a systematic review and meta-analysis. Br J Sports Med 50:292–297 [PubMed: 26626271]
4. Kay T, Harrington DE, Adams R et al. (1993) Definition of mild traumatic brain injury. J Head Trauma Rehabil 8:86–87
5. Guo X, Edmed SL, Anderson V, Kenardy J (2017) Neurocognitive predictors of posttraumatic stress disorder symptoms in children 6 months after traumatic brain injury: a prospective study. Neuropsychology 31:84–92 [PubMed: 27617636]
6. Tkachenko N, Singh K, Hasanaj L et al. (2016) Sleep disorders associated with mild traumatic brain injury using Sport Concussion Assessment Tool 3. Pediatr Neurol 57:46–50.e1 [PubMed: 26795630]
7. Ellis MJ, Ritchie LJ, Koltek M et al. (2015) Psychiatric outcomes after pediatric sports-related concussion. J Neurosurg Pediatr 16:709–718 [PubMed: 26359916]

8. Buttram SDW, Garcia-Filion P, Miller J et al. (2015) Computed tomography vs. magnetic resonance imaging for identifying acute lesions in pediatric traumatic brain injury. Hosp Pediatr 5:79–84 [PubMed: 25646200]
9. Eierud C, Craddock RC, Fletcher S et al. (2014) Neuroimaging after mild traumatic brain injury: review and meta-analysis. Neuroimage Clin 4:283–294 [PubMed: 25061565]
10. Smits M, Houston GC, Dippel DWJ et al. (2011) Microstructural brain injury in post-concussion syndrome after minor head injury. Neuroradiology 53:553–563 [PubMed: 20924757]
11. Babcock L, Yuan W, Leach J et al. (2015) White matter alterations in youth with acute mild traumatic brain injury. J Pediatr Rehabil Med 8:285–296 [PubMed: 26684069]
12. Roberts RM, Mathias JL, Rose SE (2014) Diffusion tensor imaging (DTI) findings following pediatric non-penetrating TBI: a meta-analysis. Dev Neuropsychol 39:600–637 [PubMed: 25470224]
13. Sporns O, Tononi G, Kötter R (2005) The human connectome: a structural description of the human brain. PLOS Comput Biol 1:e42 [PubMed: 16201007]
14. Jbabdi S, Behrens TEJ, Smith SM (2010) Crossing fibres in tract-based spatial statistics. Neuroimage 49:249–256 [PubMed: 19712743]
15. Calamante F, Tournier J-D, Jackson GD, Connelly A (2010) Track-density imaging (TDI): super-resolution white matter imaging using whole-brain track-density mapping. Neuroimage 53:1233–1243 [PubMed: 20643215]
16. Calamante F, Tournier J-D, Heidemann RM et al. (2011) Track density imaging (TDI): validation of super resolution property. Neuroimage 56:1259–1266 [PubMed: 21354314]
17. Payabvash S, Palacios EM, Owen JP et al. (2019) White matter connectome edge density in children with autism spectrum disorders: potential imaging biomarkers using machine-learning models.. Brain Connect 9:209–220 [PubMed: 30661372]
18. Owen JP, Wang MB, Mukherjee P (2016) Periventricular white matter is a nexus for network connectivity in the human brain. Brain Connect 6:548–57 [PubMed: 27345586]
19. Owen JP, Chang YS, Mukherjee P (2015) Edge density imaging: mapping the anatomic embedding of the structural connectome within the white matter of the human brain. Neuroimage 109:402–17 [PubMed: 25592996]
20. King NS, Crawford S, Wenden FJ et al. (1995) The Rivermead Post Concussion Symptoms Questionnaire: a measure of symptoms commonly experienced after head injury and its reliability. J Neurol 242:587–592 [PubMed: 8551320]
21. Beers SR, Wisniewski SR, Garcia-Filion P et al. (2012) Validity of a pediatric version of the Glasgow Outcome Scale–Extended. J Neurotrauma 29:1126–1139 [PubMed: 22220819]
22. Baker DA, Connery AK, Kirk JW, Kirkwood MW (2014) Embedded performance validity indicators within the California Verbal Learning Test, children's version. Clin Neuropsychol 28:116–127 [PubMed: 24229006]
23. Fan J, McCandliss BD, Sommer T et al. (2002) Testing the efficiency and independence of attentional networks. J Cogn Neurosci 14:340–347 [PubMed: 11970796]
24. Haacke EM, Duhaime AC, Gean AD et al. (2010) Common data elements in radiologic imaging of traumatic brain injury. J Magn Reson Imaging 32:516–543 [PubMed: 20815050]
25. Smith SM (2002) Fast robust automated brain extraction. Hum Brain Mapp 17:143–155 [PubMed: 12391568]
26. Jenkinson M, Bannister P, Brady M, Smith S (2002) Improved optimization for the robust and accurate linear registration and motion correction of brain images. Neuroimage 17:825–841 [PubMed: 12377157]
27. Fischl B, Salat DH, van der Kouwe AJW et al. (2004) Sequence-independent segmentation of magnetic resonance images. Neuroimage 23:S69–S84 [PubMed: 15501102]
28. Desikan RS, Segonne F, Fischl B et al. (2006) An automated labeling system for subdividing the human cerebral cortex on MRI scans into gyral based regions of interest. Neuroimage 31:968–980 [PubMed: 16530430]
29. Behrens TE, Berg HJ, Jbabdi S et al. (2007) Probabilistic diffusion tractography with multiple fibre orientations: what can we gain? Neuroimage 34:144–155 [PubMed: 17070705]

30. Wakana S, Jiang H, Nagae-Poetscher LM et al. (2004) Fiber tract-based atlas of human white matter anatomy. Radiology 230:77–87 [PubMed: 14645885]
31. Benjamini Y, Hochberg Y (1995) Controlling the false discovery rate: a practical and powerful approach to multiple testing. R Stat Soc 57:289–300
32. Toga AW, Thompson PM (2001) The role of image registration in brain mapping. Image Vis Comput 19:3–24 [PubMed: 19890483]
33. Georgieva P, De la Torre F (2013) Robust principal component analysis for brain imaging In: Mladenov V, Koprinkova-Hristova P, Palm G et al. (eds) Artificial neural networks and machine learning — ICANN 2013. Springer, Berlin, pp 288–295
34. Abdullah N, Ngah UK, Aziz SA (2011) Image classification of brain MRI using support vector machine. IEEE, pp 242–247
35. Zou KH, O'Malley AJ, Mauri L (2007) Receiver-operating characteristic analysis for evaluating diagnostic tests and predictive models. Circulation 115:654–657 [PubMed: 17283280]
36. Habeck C, Stern Y, Alzheimer's Disease Neuroimaging Initiative (2010) Multivariate data analysis for neuroimaging data: overview and application to Alzheimer's disease. Cell Biochem Biophys 58:53–67 [PubMed: 20658269]
37. Jenkinson M, Beckmann CF, Behrens TEJ et al. (2012) FSL. Neuroimage 62:782–790 [PubMed: 21979382]
38. Holmes CJ, Hoge R, Collins L et al. (1998) Enhancement of MR images using registration for signal averaging. J Comput Assist Tomogr 22:324–333 [PubMed: 9530404]
39. Levin HS, Wilde EA, Hanten G et al. (2011) Mental state attributions and diffusion tensor imaging after traumatic brain injury in children. Dev Neuropsychol 36:273–287 [PubMed: 21462007]
40. Ewing-Cobbs L, Prasad MR, Swank P et al. (2008) Arrested development and disrupted callosal microstructure following pediatric traumatic brain injury: relation to neurobehavioral outcomes. Neuroimage 42:1305–1315 [PubMed: 18655838]
41. Wozniak J, Krach L, Ward E et al. (2007) Neurocognitive and neuroimaging correlates of pediatric traumatic brain injury: a diffusion tensor imaging (DTI) study. Arch Clin Neuropsychol 22:555–568 [PubMed: 17446039]
42. Fakhran S, Yaeger K, Collins M, Alhilali L (2014) Sex differences in white matter abnormalities after mild traumatic brain injury: localization and correlation with outcome. Radiology 272:815–823 [PubMed: 24802388]
43. McCauley SR, Wilde EA, Bigler ED et al. (2011) Diffusion tensor imaging of incentive effects in prospective memory after pediatric traumatic brain injury. J Neurotrauma 28:503–516 [PubMed: 21250917]
44. Oni MB, Wilde EA, Bigler ED et al. (2010) Diffusion tensor imaging analysis of frontal lobes in pediatric traumatic brain injury. J Child Neurol 25:976–984 [PubMed: 20332386]
45. Wilde EA, Bigler ED, Haider JM et al. (2006) Vulnerability of the anterior commissure in moderate to severe pediatric traumatic brain injury. J Child Neurol 21:769–776 [PubMed: 16970884]
46. Cicuendez M, Castaño-León A, Ramos A et al. (2017) Prognostic value of corpus callosum injuries in severe head trauma. Acta Neurochir 159:25–32 [PubMed: 27796652]
47. Jellison BJ, Field AS, Medow J et al. (2004) Diffusion tensor imaging of cerebral white matter: a pictorial review of physics, fiber tract anatomy, and tumor imaging patterns. AJNR Am J Neuroradiol 25:356–369 [PubMed: 15037456]
48. Mayer AR, Ling JM, Yang Z et al. (2012) Diffusion Abnormalities in pediatric mild traumatic brain injury. J Neurosci 32:17961–17969 [PubMed: 23238712]
49. DeMaster D, Johnson C, Juranek J, Ewing-Cobbs L (2017) Memory and the hippocampal formation following pediatric traumatic brain injury. Brain Behav 7:e00832 [PubMed: 29299377]
50. Wu TC, Wilde EA, Bigler ED et al. (2010) Longitudinal changes in the corpus callosum following pediatric traumatic brain injury. Dev Neurosci 32:361–373 [PubMed: 20948181]
51. Mioni G, Grondin S, Stablum F (2014) Temporal dysfunction in traumatic brain injury patients: primary or secondary impairment? Front Hum Neurosci 8:269 [PubMed: 24817847]

52. Buethe J, Nazarian J, Kalisz K, Wintermark M (2016) Neuroimaging wisely. AJNR Am J Neuroradiol 37:2182–2188 [PubMed: 27282861]

53. Wintermark M, Sanelli PC, Anzai Y et al. (2015) Imaging evidence and recommendations for traumatic brain injury: advanced neuro- and neurovascular imaging techniques. AJNR Am J Neuroradiol 36:E1–E11 [PubMed: 25424870]

54. Bach M, Laun FB, Leemans A et al. (2014) Methodological considerations on tract-based spatial statistics (TBSS). Neuroimage 100:358–369 [PubMed: 24945661]

55. Peled S, Yeshurun Y (2001) Superresolution in MRI: application to human white matter fiber tract visualization by diffusion tensor imaging. Magn Reson Med 45:29–35 [PubMed: 11146482]

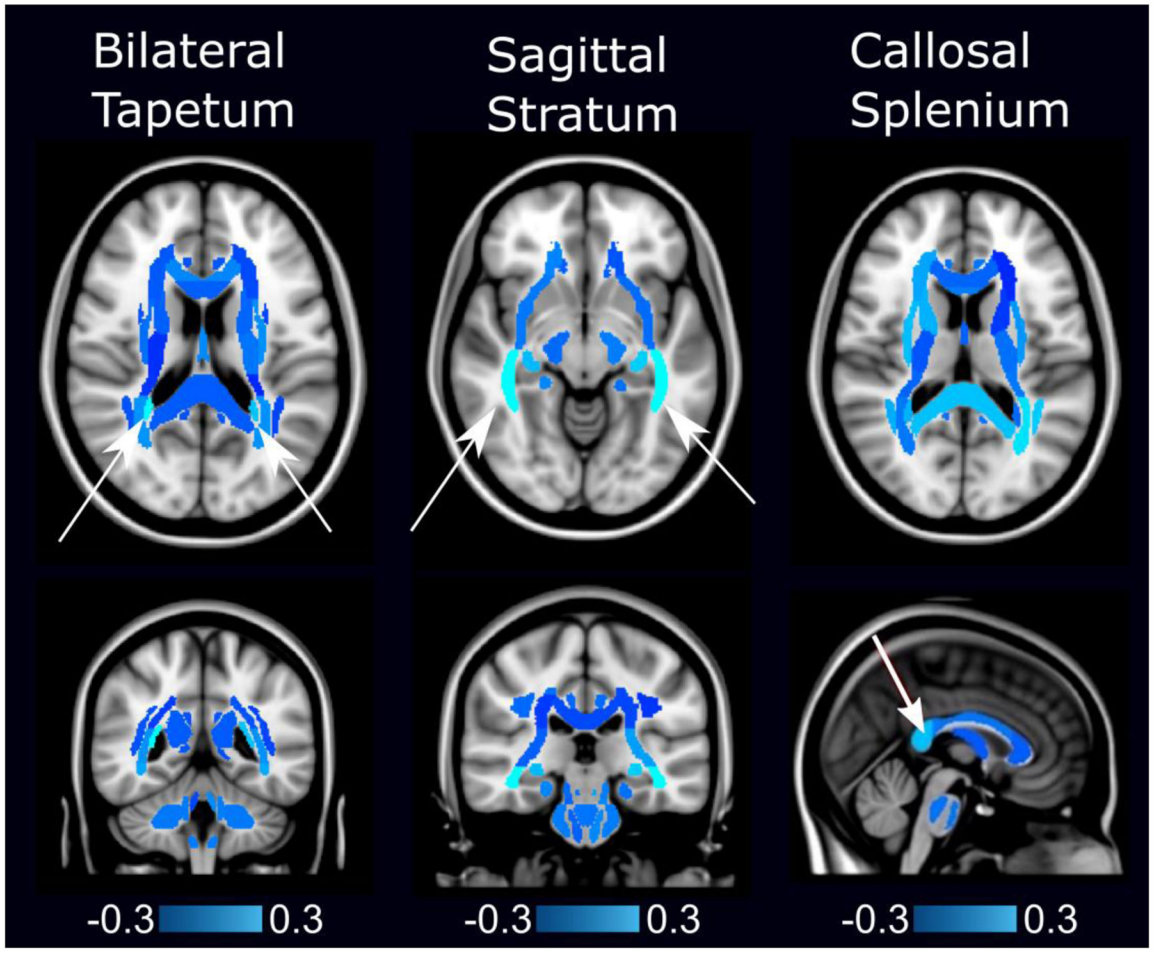

Fig. 1.

Edge density imaging map shows specific white matter regions of group results (*arrows*) that distinguish children with mild traumatic brain injury (TBI) from controls, projected onto the standard single-subject Montreal Neurological Institute (MNI) brain template [38]. (Table 1 details participant demographics.) In this figure, light blue regions are associated with higher edge density in controls (mean age 14.2 years, 50% female) compared to those with mild TBI (mean age 14.2 years, 36% female). Dark blue regions are associated with the opposite. The bilateral tapetum, sagittal stratum, and the splenium of the corpus callosum have higher edge densities in controls compared to children with mild TBI, and these differences are the most predictive features for accurate classification

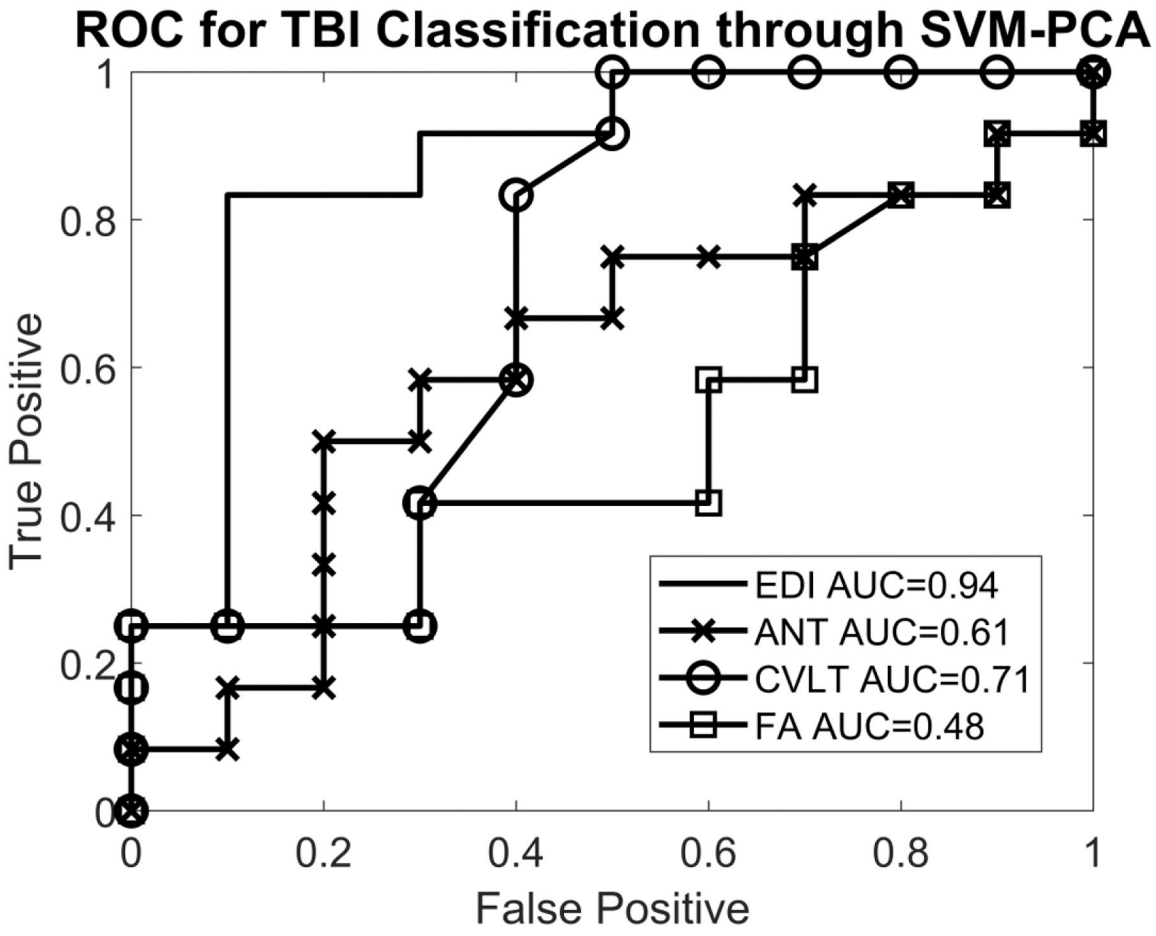

Fig. 2.

Receiver operating characteristic (ROC) curve for support vector machine (SVM)–principal component analysis (PCA) predictors in differentiating pediatric mild traumatic brain injury (TBI) cases from controls. SVM and PCA were used to generate a "TBI predictor" under a leave-one-out cross-validation, and the ROC curves based on these predictors are plotted here. For edge density imaging, the area under the curve (AUC) was 94%. Fractional anisotropy (FA) values resulted in an AUC of 48% in distinguishing children with mild TBI from controls. Neurocognitive testing yielded an AUC of distinguishing children with mild TBI from controls ranging from 61% with the Attention Network Task (ANT) to 71% with the California Verbal Learning Test (CVLT). No statistically significant correlations were observed between neurocognitive test results and either the diffusion tensor imaging (DTI) scalars or the edge density imaging maps

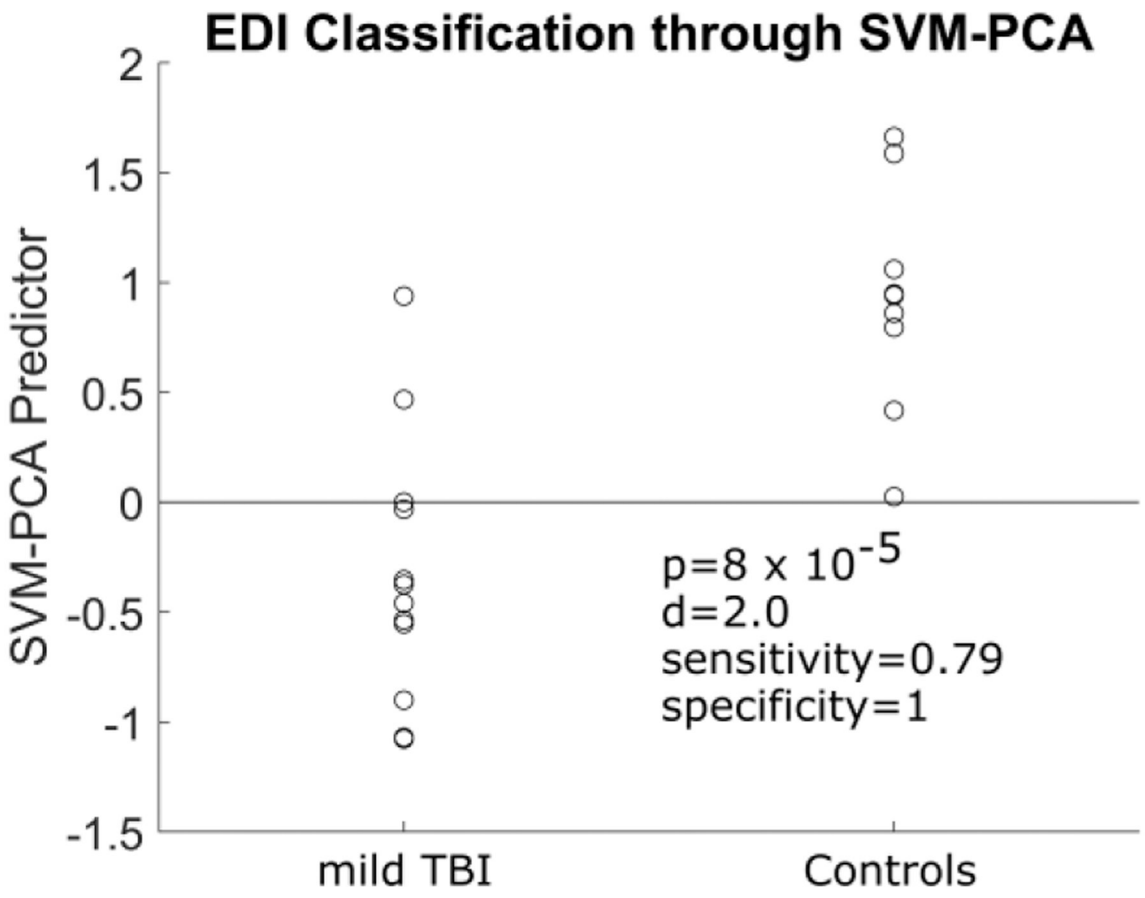

Fig. 3.

Individual control and mild traumatic brain injury (TBI) cases and their distances from the support vector machine hyperplane (*gray line*). A positive distance in this figure is noted with controls, and a negative distance with mild TBI cases. *EDI* edge density imaging, *SVM-PCA* support vector machine–principal component analysis

Table 1

Therapeutic resources for attention improvement using neuroimaging in traumatic brain injury (TRAIN-TBI) study subject characteristics

		Controls (*n*=10)		Pediatric mild TBI (*n*=14)	
		χ±σ	**Count (*n*)**	**χ±σ (*P*-value)[a]**	**Count (*n*)**
Age		14.0*a*±1.7		14.2*a*+1.6	
Gender	Male		5*a*		9*a*
	Female		5*a*		5*a*
Handedness	Right		9*a*		14
	Left		1*a*		0
Years of education		8.6*a*±1.6		8.1*a*±1.9	
ANT conflict		80.6*a*±19.1		100.4*a*±32.1	
ANT orienting		56.9*a*±20.1		45.5*a*±19.1	
ANT alerting		33.0*a*±20.8		54.5*a*±39.1	
ANT reaction time		555.1*a*±70.2		566.0*a*±102.2	
CVLT long delayed cued recall		14*a*±1.1		12_b±0.25 **(*P*=0.004)**	
CVLT long delayed free recall		14*a*±1.2		12_b±0.46 **(*P*=0.02)**	
CVLT short delayed free recall		13*a*±0.7		12*a*±0.5	
CVLT Trials 1 to 5 T score		62*a*±6.6		56_b±5.7 **(*P*=0.03)**	

ANT Attention Network Task, *CVLT* California Verbal Learning Test, *TBI* traumatic brain injury

[a]Values in the same row and sub-table not sharing the same subscript are significantly different at $P<0.05$ in the two-sided test of equality for column proportions. Cells with no subscript were not included in the test. Tests assume equal variances